



HAL
open science

Hydrogen Silsesquioxane-Based Nanofluidics

Sathyanarayanan Punniyakoti, Ragavendran Sivakumarasamy, Francois Vaurette, Pierre Joseph, Katsuhiko Nishiguchi, Akira Fujiwara, Nicolas Clément

► **To cite this version:**

Sathyanarayanan Punniyakoti, Ragavendran Sivakumarasamy, Francois Vaurette, Pierre Joseph, Katsuhiko Nishiguchi, et al.. Hydrogen Silsesquioxane-Based Nanofluidics. *Advanced Materials Interfaces*, 2017, 4 (7), pp.1601155. 10.1002/admi.201601155 . hal-01701361

HAL Id: hal-01701361

<https://laas.hal.science/hal-01701361>

Submitted on 5 Feb 2018

HAL is a multi-disciplinary open access archive for the deposit and dissemination of scientific research documents, whether they are published or not. The documents may come from teaching and research institutions in France or abroad, or from public or private research centers.

L'archive ouverte pluridisciplinaire **HAL**, est destinée au dépôt et à la diffusion de documents scientifiques de niveau recherche, publiés ou non, émanant des établissements d'enseignement et de recherche français ou étrangers, des laboratoires publics ou privés.

Advanced Materials Interfaces

Hydrogen Silsesquioxane-based Nanofluidics

--Manuscript Draft--

Manuscript Number:	
Full Title:	Hydrogen Silsesquioxane-based Nanofluidics
Article Type:	Full Paper
Section/Category:	
Keywords:	Nanofluidics; HSQ; 3D Nanofluidics; extremely slow evaporation rate
Corresponding Author:	nicolas clement IEMN-LILLE1 VILLENEUVE D'AS, FRANCE
Additional Information:	
Question	Response
Corresponding Author Secondary Information:	
Corresponding Author's Institution:	IEMN-LILLE1
Corresponding Author's Secondary Institution:	
First Author:	nicolas clement
First Author Secondary Information:	
Order of Authors:	nicolas clement Sathya Punniyakoti Ragavendran Sivakumarasamy Francois Vaurette Pierre Joseph Katsuhiko Nishiguchi Akira Fujiwara
Order of Authors Secondary Information:	
Abstract:	Nanofluidics show great promise for the control of small volumes and single molecules, especially for biological and energy applications. To build up more and more complex nanofluidics systems, a versatile and reproducible fabrication technique with nanometer precision alignment is desirable. In this article, we present two e-beam lithography methods to fabricate nanofluidic channels based on hydrogen silsesquioxane (HSQ), a high-resolution negative-tone inorganic resist. The robustness and versatility of the fabrication processes are demonstrated on silicon, glass and flexible substrates. The high precision ability is illustrated with nanometric alignment of nanofluidic channels on gold nanoparticles and nanotransistor sensors, as well as for 3D nanofluidics prototyping. Furthermore, we noticed an unexpected extremely slow water evaporation rate (~1 week for 300µm-long nano-channels). This feature enables a simple and reliable manipulation of nanofluidic chips for various studies.

DOI: 10.1002/ ((please add manuscript number))

Article type: Full Paper

Hydrogen Silsesquioxane-based Nanofluidics

*Sathyanarayanan Punniyakoti, Ragavendran Sivakumarasamy, Francois Vaurette, Pierre Joseph, Katsuhiko Nishiguchi, Akira Fujiwara, and Nicolas Clément**

Dr. S. Punniyakoti,

IEMN-CNRS, Avenue Poincaré, 59652, Villeneuve d'Ascq, France; Present address: Centre for Nanotechnology Research, VIT University, Vellore, 632 014, Tamil Nadu, India

Dr. R. Sivakumarasamy, Dr. F. Vaurette

IEMN-CNRS, Univ. of Lille, Avenue Poincaré, 59652, Villeneuve d'Ascq, France

Dr. P. Joseph

LAAS-CNRS, Université de Toulouse, CNRS, Toulouse, France

Dr. K. Nishiguchi, A. Fujiwara

NTT Basic Research Laboratories, 3-1, Morinosato Wakamiya, Atsugi-shi, 243-0198, Japan

Dr. N. Clément

IEMN-CNRS, Univ. of Lille, Avenue Poincaré, 59652, Villeneuve d'Ascq, France and NTT Basic Research Laboratories, 3-1, Morinosato Wakamiya, Atsugi-shi, 243-0198, Japan

E-mail: nicolas.clement@lab.ntt.co.jp

Keywords: Nanofluidics, HSQ, 3D Nanofluidics, extremely slow evaporation rate

Nanofluidics show great promise for the control of small volumes and single molecules, especially for biological and energy applications. To build up more and more complex nanofluidics systems, a versatile and reproducible fabrication technique with nanometer precision alignment is desirable. In this article, we present two e-beam lithography methods to fabricate nanofluidic channels based on hydrogen silsesquioxane (HSQ), a high-resolution negative-tone inorganic resist. The robustness and versatility of the fabrication processes are demonstrated on silicon, glass and flexible substrates. The high precision ability is illustrated with nanometric alignment of nanofluidic channels on gold nanoparticles and nanotransistor sensors, as well as for 3D nanofluidics prototyping. Furthermore, we noticed an unexpected extremely slow water evaporation rate (~1 week for 300µm-long nano-channels). This feature enables a simple and reliable manipulation of nanofluidic chips for various studies.

1. Introduction

1
2 Thanks to its unique features at the nanoscale, nanofluidics, the study and application
3
4 of fluid flow in nanochannels/nanopores with at least one characteristic size smaller than 100
5
6 nm, has enabled the occurrence of many interesting transport phenomena and has shown great
7
8 potential in both bio- and energy-related fields.^[1-5] The unprecedented growth of this research
9
10 field is related to the rapid development of micro/nanofabrication techniques. Several
11
12 methods have been developed thus far to afford the fabrication of nanochannels such as
13
14 optical, e-beam, nanoimprint lithography with sacrificial layers or etching^[1, 6-10]. Another
15
16 alternative is the use of nanoporous materials.^[11, 12] Although these different methods are
17
18 relatively simple, many of them are not compatible with a low-temperature process (e.g. for
19
20 plastic substrates or organic devices), or do not offer good alignment ability on patterned
21
22 substrates for rapid prototyping of complex nanofluidic systems (e.g. for hybrid
23
24 nanofluidics/nanosensor devices or 3D nanochannels fabrication).

25
26
27
28
29
30
31 Si-based inorganic-organic polymers with a general structure of $[R_xSiO_y]_n$ (R is a
32
33 hydrocarbon group) have the advantage of being processed at low temperature. However, they
34
35 cannot be aligned at nanometer scale, and they have a small Young modulus which prevents
36
37 their use in nanofluidics. Hard PDMS (a PDMS engineered to have a higher mechanical
38
39 modulus of ~8 MPa) has been successfully used for nanofluidics,^[13,14] but its Young modulus
40
41 remains small. Polysilsesquioxane (PSQ) has a much higher Young modulus (800 MPa).^[15] It
42
43 has been successfully used as a simple sealing method,^[16] but it cannot be directly prototyped.
44
45 Finally, Hydrogen Silsesquioxane (HSQ: Fox 16, Dow Corning) can be processed at low
46
47 temperature, with the high precision alignment provided by e-beam lithography, and provides
48
49 an additional advantage of planarity. It has often been used in nanoelectronics as a mask
50
51 before silicon etching thanks to its high resolution (<10 nm). It can be almost densified to
52
53 SiO₂ after plasma or electron-beam exposition,^[17-19] and has also been used for 3D
54
55 prototyping of photonic crystals^[20], or for the fabrication of dielectric nanoantennas^[21].

1 However, except its use as a high resolution mold^[22] or as channels arising from the collapse
2 of thin HSQ walls,^[23] the unique advantages provided by this material have not been exploited
3
4 to demonstrate a potential use in nanofluidics.
5
6

7
8
9 Here, we show that HSQ can be used as a structuring material for nanofluidics applications.
10
11 We take advantage of the direct HSQ prototyping at nanometer scale and its high planarity to
12 demonstrate two simple and versatile ways of fabricating nanofluidic channels. In particular,
13
14 we show the possibility to fabricate 3D stacked layers, and to align nanochannels on
15
16 nanostructured surfaces such as gold nanoparticles or nanotransistor biosensors. Limitations
17
18 and related solutions specific to the use of HSQ for nanofluidics applications are presented as
19
20 a guide-line for a practical use of HSQ in nanofluidics. We also evidence an extremely slow
21
22 evaporation rate of water inside the channels covered by HSQ, an unexpected feature that
23
24 significantly simplifies microscope studies of chips composed of nanofluidics channels.
25
26
27
28
29
30

31 32 **2. Nanofluidic channels fabricated by direct HSQ prototyping (First approach)**

33
34 The first approach is based on direct prototyping of HSQ, being used as a negative tone
35
36 electron beam resist. Technological steps for the proposed approach are summarized in Figure
37
38
39
40 1a. The starting substrate is an n-type bulk silicon wafer covered with native oxide. If
41
42 necessary, alignment markers are made using standard photolithography. After substrate
43
44 dehydration (at 180°C for 10 minutes), HSQ is spin-coated to get an 850-nm-thick layer. Then,
45
46 the HSQ is exposed to e-beam and developed in tetramethyl ammonium hydroxide (TMAH)-
47
48 25% solution for 90 seconds. It is then baked on a hot plate for 30 minutes at 110°C followed
49
50
51 by 30 minutes annealing at 180°C to get robust hydrophilic and transparent nanofluidic
52
53 channel walls. Using an aligned and patterned Polydimethylsiloxane (PDMS) layer,^[24]
54
55
56 nanofluidic channels are sealed and the connection to microfluidic channels is established.
57
58
59 The distance between walls on access leads has to be small enough (below 3 μm) and sharp
60
61
62
63
64
65

1
2
3
4
5
6
7
8
9
10
11
12
13
14
15
16
17
18
19
20
21
22
23
24
25
26
27
28
29
30
31
32
33
34
35
36
37
38
39
40
41
42
43
44
45
46
47
48
49
50
51
52
53
54
55
56
57
58
59
60
61
62
63
64
65

enough to avoid bonding of PDMS to the bottom of the channels. On the other hand, at the either ends of the HSQ walls, a smooth slope is required for proper PDMS/HSQ sealing in order to avoid undesired leakage. This 3D prototyping can be achieved by using different e-beam doses within a single writing step (less exposed areas appear thinner after HSQ resist development (see Supplementary Figs.1,2 for more details)). Figure 1b shows a Scanning Electron Microscope (SEM) image of the fabricated HSQ structure composed of parallel large channels with constrictions (nanofluidic channels) and also the smooth slope at the extreme ends of the array. The e-beam writing time was approximately 1 minute and the average roughness on the top of HSQ surface is 0.7 nm. A smooth slope of 10° on HSQ has been obtained from ten 90 nm-thick, 500 nm-wide stairs obtained from 10 different exposure doses. The average nanofluidic channel width, obtained from 37 channels, is 97 nm +/- 3.7 nm (Figure 1c) which highlights the reliability of the proposed technology. Nevertheless, we observe that 15% of the channels are out of this statistics that we attribute to the high aspect ratio (HSQ thickness vs channel width) required for nanofluidics application. All channels remain within an error of 25 nm above the average width. There is a tradeoff between the HSQ thickness and the channel width. For example, Grigorescu et al.^[18] reported a 10 nm gap for a 10-nm-thick HSQ (aspect ratio of 1). Such a small layer thickness is well-suited when HSQ is being used as a mask for the nanofabrication purposes. It is however not compatible with the present HSQ-based nanofluidics, mainly because PDMS can partly bind to the bottom of the channel in the 2 or 3 μm access leads. This is illustrated in Supplementary Fig.3 for a 300-nm-thick HSQ layer. We found that 400 nm can be considered as a minimum thickness and 850 nm a good tradeoff for high resolution, high reliability (no PDMS bonding in the channel), and reduced pressure drop (3-μm-wide access leads can be used at this HSQ layer thickness). We also noticed that there is no major difference in channel width resolution between 400 nm and 850 nm thick HSQ channels. Our best result with a 850-nm-thick HSQ layer is 74 nm (aspect ratio of 12, see Supplementary Fig.4). If a smaller gap is required for

1 some applications (at high ionic strength, a 100-nm-wide nanochannel becomes too large
2 compared to the Debye screening length), this can be achieved by using atomic layer
3 deposition (ALD) (see Supplementary Fig.5 for channel width reduction by Al₂O₃ ALD). This
4 combined HSQ/ALD approach is also promising for the development of vertical nanofluidics
5 transistors as Pt can also be deposited by ALD (Supplementary Fig.5).
6
7
8
9
10

11 Figure 2 illustrates the versatility of the technique with three different substrates:
12 silicon, glass slide and flexible polyethylene naphthalate (PEN) respectively. On silicon
13 substrates, in complement to Figure 1, Figures 2a, 2b and 2c show the HSQ patterned area
14 (150 μm large and 300 μm long), the PDMS-sealed nanofluidics channels before water filling,
15 and the different stages of water filling under a given pressure of 3 bars. It confirms that
16 nanofluidic channels can be successfully operated with this technology. Although difference
17 in filling times (up to tens of seconds) is observed, all channels can be filled under the same
18 pressure, which is consistent with the small dispersion in channel widths observed by SEM.
19 The process can be transposed to other substrates by simply evaporating a thin layer of
20 Germanium (~ 5 nm) on top of the HSQ before e-beam lithography so as to evacuate charges.
21 After exposure, the germanium layer was removed with a 1:1 solution of H₂O₂:H₂O during
22 ~1min. Then, the process is the same as on silicon. Figure 2d, 2e and 2f show HSQ patterned
23 areas on a glass slide and the complete filling of fluorescent marked DNA molecules inside
24 the nanofluidic channels.^[14,25] Figure 2g and 2h indicate that similar results can also be
25 obtained on a flexible substrate. In that particular case, the flexible substrate was first fixed on
26 silicon substrate by mean of a droplet of PDMS prior spin coating.
27
28
29
30
31
32
33
34
35
36
37
38
39
40
41
42
43
44
45
46
47
48
49
50
51
52

53 **3. Fabrication of nanochannels with extremely slow evaporation rate by direct** 54 **prototyping of AZnLof and HSQ resists (Second approach)** 55 56 57 58 59 60 61 62 63 64 65

1 We also propose a second HSQ-based approach using the conventional sacrificial layer
2 method (see Figure 3). These sacrificial layers are usually either metal layers^[26-30] or positive
3
4 resists like PMMA^[8] and both of these have some drawbacks. The former one involves
5
6 removal of metal layers at the end of the process which is usually difficult and requires few
7
8 hours.^[31, 32] The later one involves writing of large areas, which is not the optimum solution.
9
10 Recently, it was demonstrated that AZnLof, usually used for optical lithography, could also
11
12 be patterned by e-beam with very high resolution.^[33] We spin-coated 100 nm-thick diluted
13
14 resist AZnLof 2020 in PGMEA (1:3 ratio), and defined nanochannels by e-beam, prior to
15
16 HSQ deposition (Figure 3a). Both lateral and vertical dimensions can be set down to ~100 nm
17
18 (Figure 3b). We noticed that an annealing step at 170°C enabled optimization of the resist
19
20 roughness leading to a perfect half-cylinder (Figure 3b). After HSQ deposition and baking, a
21
22 piranha solution (H₂SO₄/H₂O₂:2/1) was used to dissolve and remove the embedded AZnLof
23
24 resist by gentle agitation (50 rpm) for 30 minutes, leaving channels with clean and smooth
25
26 inner surfaces. The remaining piranha in the channels was replaced finally by DI water rinse
27
28 under agitation. The advantages of HSQ to make the channel rather than other deposition
29
30 methods such as sputtering, are to take advantage of its planarity and get rid of extra
31
32 lithography and etching steps that can be complicated, in particular on patterned surfaces. It
33
34 will be illustrated in the next section. We also experienced a difficulty for removing the
35
36 AZnLof layer when it is covered with another oxide such as an Al₂O₃ deposited by ALD
37
38 before HSQ deposition.

39
40
41 Interestingly, we noticed that water in the channels remained for at least one week
42
43 without noticeable evaporation with inlets/outlets open to air as presented in Figure 3c (no
44
45 PDMS bonding in this approach); whereas in the first approach with direct HSQ prototyping,
46
47 the complete evaporation was observed in few minutes. These experiments have been
48
49 performed in clean room at a fixed temperature of 21°C and a humidity ratio of approximately
50
51 50%. It was previously shown that roughness or section shape (square vs circular) plays a
52
53
54
55
56
57
58
59
60
61
62
63
64
65

critical role in the evaporation in microfluidic channels,^[34-40] and consensus seems to have been reached that surface cleanliness plays an important role.^[41] However, typical evaporation times in micro- or nano- fluidic channels are in the minute range^[34-42] (or in the range of mm per minute), which is more than 4 orders of magnitude faster than in the present study. Sole consideration of the steady-state vapor diffusion governed by the Laplace equation^[43] should lead to evaporation times in the second or minute range with or without consideration of evaporation-induced cavitation effects.^[37] The present structure has a small roughness which may increase the evaporation time as already discussed in the literature,^[34] but cannot fully explain the extremely slow evaporation rate observed. **A full understanding of the underlying mechanisms requires a dedicated experimental and theoretical study as in refs. ^[37,44]. We suggest that the experimentally observed slow evaporation rate could be related either to the absence of impurities due to the non-exposure to air, or to an hydrophobic/hydrophilic transition at nanofluidic channels inlets/outlets^[45,46] (HSQ hydrophobicity depends on the e-beam dose^[22] which is expected to be weaker at channel ends), or eventually to nanoporosity in HSQ.** This extremely slow evaporation rate is of practical interest to simplify setups for microscopy experiments (see Figure.3d showing a fluorescent image of nanofluidic channels filled with marked DNA).

4. 3D Nanofluidics and nanometric precision alignment

In a similar manner as for the fabrication of photonic crystals,^[20] the good alignment ability **and the unique planarity provided by HSQ,** enable to stack these layers together to make 3D nanofluidic channels (Figure 4a and 4b), a key step for highly integrated and multiplexed nanofluidics. It was achieved here by repeating AZnLof patterning and HSQ deposition. Figure 4b, inset, shows two levels of channels with interconnect openings (vias) between the top and bottom layers, **and the planar upper surface of the HSQ layer (images of the various steps are shown in Supplementary Fig.6. Vias were achieved by performing e-beam**

1 lithography on PMMA resist (5% 950K, 3 μ m-thick) prior to reactive ion etching of HSQ by
2 CF₄/CHF₃ plasma. Several design rules have to be respected for HSQ-based 3D nanofluidics.
3
4 A thin HSQ layer is required because of the non-uniform reactive plasma etching rate
5
6 between vias centers and sides, which render difficult the uniform etching down to the 100
7
8 nm-thick underlayer of AZnLoF (Supplementary Fig.7a,b). An optimum HSQ-layer thickness
9
10 (\approx 500 nm) was selected based on the observation that nanofluidic channels collapse, either
11
12 during HSQ baking or during AZnLoF removal, for HSQ layer thicknesses below 400 nm
13
14 (Supplementary Fig.7b). This effect is channel-width dependent. In particular, for channels
15
16 wider than 4 μ m, channels are systematically collapsed, independently on the HSQ layer
17
18 thickness. In the 500-nm-thick HSQ layer configuration, 500-nm-wide vias could be achieved.
19
20 Smaller vias (e.g. 200 nm or smaller), require significant optimization of the etching rate and
21
22 suffer from reproducibility. Larger vias affect the uniformity of the second layer of AZnLoF
23
24 that partly falls into the via (Supplementary Fig.7), and results in a clogged hole after the
25
26 deposition of a second layer of HSQ. With these design rules in mind, the process is very
27
28 robust and reproducible.
29
30
31
32
33
34
35

36 Although some previous reports have successfully shown the possibility of 3D
37
38 nanofluidics^[47-49], the degree of control/precision proposed with HSQ-based nanofluidics
39
40 (channels crossing) brings new perspectives toward well controlled large-scale integrated
41
42 nanofluidics or hybrid devices. When the surface is initially patterned, the combination of
43
44 nanometric precision alignment and planarity are required. For example, single-crystal Au
45
46 nanoparticles (fabricated by e-beam lithography and thermal annealing), or nanoscale
47
48 transistor sensors, have been successfully used in the fields of molecular electronics^[50-53]
49
50 electrochemistry^[53,54] and single-molecule or single-charge-sensitive biosensors^[55-57].
51
52
53
54
55 Nanofluidics could be a very attractive approach to provide an upper electrode made of liquid
56
57 metal^[58] for high-frequency molecular electronics^[53], to reduce parasitic capacitance in
58
59 nanoelectrochemistry, or simply to focus analytes on top of nanoscale biosensors. Figure 5
60
61
62
63
64
65

shows the ability to fabricate such structures on Au nanoparticles and 50 nm-thick nanoscale transistor biosensors without any further complexity arising from the patterned surfaces.

5. Conclusion

We proposed the demonstration of a well-controlled and versatile technique for the fabrication of nanofluidic channels with nanometric precision alignment based on HSQ. The first approach requires only a single, small area writing step, and enables nanometric precision alignment. In the second approach, a conventional sacrificial layer approach was exploited for the fabrication of ~100 nm diameter half-pipe HSQ nanofluidics channels together with nanometric precision alignment and 3D nanofluidics demonstration. The proposed reliable approaches provides a pathway for the development of more and more complex nanofluidic systems including the interfacing of nanofluidics with nanoscale sensors, while the extremely slow evaporation rate brings simplicity for the characterizations or applications and new perspectives for basic research in nanofluidics.

6. Experimental Section

Si mold:

S1818 resist (Microposit©) was spin-coated at 2500 rpm with an acceleration of 1000 rpm for 12 s. Silicon was etched using reactive ion etching (RIE). The gases used for the RIE process was SF₆ and O₂ and the gas used for passivation was C₄F₈. The flow rates of SF₆, O₂, and C₄F₈ were 450, 45, and 100 standard cm³ per minute (sccm), respectively. The coil power was 1000 W. RIE had an approximate etch rate of 4 μm/min. After etching the wafers, we examined the microstructures on the wafers by optical microscopy. We stripped the remaining photoresist from the silicon wafer by immersing the wafer in EKC 265 at 60° C for 30 min, followed by immersion in acetone and isopropanol for 5 min each.

PDMS Layer Fabrication (For method 1):

1
2 A thin layer of PDMS (thickness: 200 μm) was required for the alignment protocol and for
3
4 precisely defining the holes for tubing. The uncured PDMS (mixing ratio of curing agent/
5
6 base ratio: 1/3) was spin-coated at 300 rpm for 30 s, with an acceleration rate of 100 rpm/s. It
7
8 was then cured in two steps: (i) at 65 $^{\circ}\text{C}$ for 20 min in contact with a hot plate and (ii) in a
9
10 convection oven at 120 $^{\circ}\text{C}$ for 40 min.
11
12
13

Alignment and Bonding (For method 1):

14
15
16
17 Prior to bonding, the Si chip and PDMS layer were exposed to O_2 plasma (120 W, 0.7 mbar,
18
19 180 s) and to UV-ozone for 5 min. After proper alignment and bonding with 1- μm alignment
20
21 precision,^[24] thermal annealing was performed at 120 $^{\circ}\text{C}$ for 60 min.
22
23

24
25
26 A second layer of PDMS (2 mm in thickness) was used to guide the tube and reduce the
27
28 mechanical stress at the inlet and outlet. Access holes for connecting the inlet and outlet tubes
29
30 (PTFE tubing: 0.7mm/0.3 mm outer diameter [OD]/inner diameter [ID]) were cored into the
31
32 2-mm-thick PDMS by using a 300- μm -ID needle, with an approximate distance between the
33
34 two holes of less than 1 mm.
35
36
37

Supporting Information

38
39
40 Supporting Information is available from the Wiley Online Library.
41
42
43

Acknowledgements

44
45
46 The authors would like to thank P. Tilmant and Y.Viero for discussions, D.Troadeac for FIB
47
48 cross sections, and the CPER CENIA for funding of S. Punniyakoti's post-doc and the
49
50 SINGLEMOL project from Nord Pas de Calais council for funding the process work. This
51
52 work was partially funded by the RENATECH network.
53
54
55
56

57 Received: ((will be filled in by the editorial staff))

58 Revised: ((will be filled in by the editorial staff))

59 Published online: ((will be filled in by the editorial staff))
60
61

- 1 [1] D. Xia, J. Yan, and S. Hou, *Small* **2012**, 8, 2787.
- 2 [2] W. Reisner, K. J. Morton, R. Riehn, Y. M. Wang, Z. Yu, M. Rosen, J. C. Sturm, S. Y.
- 3 Chou, E. Frey, and R. H. Austin, *Phys. Rev. Lett.*, **2005**, 94, 196101.
- 4 [3] X. Liang, K. J. Morton, R. H. Austin, and S. Y. Chou, *Nano Lett.*, **2007**, 7, 3774.
- 5 [4] W. Guo, L. Cao, J. Xia, F.-Q. Nie, W. Ma, J. Xue, Y. Song, D. Zhu, Y. Wang, and L.
- 6 Jiang, *Adv. Funct. Mater.*, **2010**, 20, 1339.
- 7 [5] D. Gillespie, *Nano Lett.*, **2012**, 12, 1410.
- 8 [6] J.M. Perry, D. Harms and S.C. Jacobson, *Small*, **2012**, 8, 1521.
- 9 [7] C. Duan, W. Wang, and Q. Xie, *Biomicrofluidics*, **2013**, 7, 026501.
- 10 [8] F. Güder, Y. Yang, M. Krüger, G. B. Stevens, and M. Zacharias, *ACS Appl. Mater.*
- 11 *Interfaces.*, **2010**, 2, 3473.
- 12 [9] Y. Wu, J. Zhou and E. Y. B. Pun, *J. MicroNanolithography MEMS MOEMS*, **2011**, 10,
- 13 049701.
- 14 [10] P. Abgrall and N. T. Nguyen, *Anal. Chem.*, **2008**, 80, 2326.
- 15 [11] D. Xia and S. R. J. Brueck, *J. Vac. Sci. Technol. B*, **2005**, 23, 2694.
- 16 [12] D. Xia, T. C. Gamble, E. A. Mendoza, S. J. Koch, X. He, G. P. Lopez, and S. R. J.
- 17 Brueck, *Nano Lett.*, **2008**, 8, 1610.
- 18 [13] H. Schmid and B. Michel, *Macromolecules*, **2000**, 33, 3042.
- 19 [14] Q. Hao, Q. He, H. Ranchon, P. Carrivain, Y. Viero, J. Lacroix, C. Blatche, E. Daran,
- 20 J.-M. Victor, and A. Bancaud, *Macromolecules*, **2013**, 46, 6195.
- 21 [15] N. Takamura, T. Gunji, H. Hatano, and Y. Abe, *J. Polym.Sci.Part.A:Polym.Chem.*,
- 22 **1999**, 37, 1017.
- 23 [16] H. Namatsu, Y. Takahashi, K. Yamazaki, T. Yamaguchi, M. Nagase, and K. Kurihara,
- 24 *J. Vac. Sci. Technol. B*, **1998**, 16, 69.
- 25 [17] J. Gu, R. Gupta, C.-F. Chou, Q. Wei, and F. Zenhausern *Lab.Chip.*, **2007**, 7, 1198.

- 1
2
3
4
5
6
7
8
9
10
11
12
13
14
15
16
17
18
19
20
21
22
23
24
25
26
27
28
29
30
31
32
33
34
35
36
37
38
39
40
41
42
43
44
45
46
47
48
49
50
51
52
53
54
55
56
57
58
59
60
61
62
63
64
65
- [18] A. E. Grigorescu, M. C. van der Krogt, C. W. Hagen, and P. Kruit, *Microelectron. Eng.*, **2007**, 84, 822.
- [19] Y. Guerfi, J.B. Doucet, and G. Larrieu, *Nanotechnology*, **2015**, 26, 425302.
- [20] L. T. Varghese, L. Fan, J. Wang, Y. Xuan, and M. Qi, *Small*, **2013**, 24, 4237.
- [21] P.R. Wiecha, A. Arbouet, C. Girard, A. Lecestre, G. Larrieu and V. Paillard, *Nat.Nano.*, **2016**, doi://10.1038/nnano.2016.224
- [22] J.A. van Kan, C.Z. Zhang, P.P. Mador, and J.R.C. van der Maarel, *Biomicrofluidics*, **2012**, 6, 036502.
- [23] S. Choi, M. Yan, and I. Adesida, *Appl.Phys.Lett.*, **2008**, 93, 163113.
- [24] R. Sivakumarasamy, K. Nishiguchi, A. Fujiwara, D. Vuillaume and N. Clement, *Anal.Methods*, **2014**, 97, 6.
- [25] W.Reisner, J.P.Beech, N.B. Larsen, H. Flyvbjerg, A. Kristensen, J.O. Tegenfeldt, *Phys.Rev.Lett.*, **2007**, 99, 058302.
- [26] G. J. Cheng, D. Pirzada, and P. Dutta, *J. MicroNanolithography MEMS MOEMS*, **2005**, 4, 013009.
- [27] H. Zeng, Z. Wan, and A. D. Feinerman, *Nanotechnology*, **2006**, 17, 3183.
- [28] J. C. T. Eijkel, J. Bomer, N. R. Tas, and A. van den Berg, *Lab. Chip*, 2004, 4, 161.
- [29] K. P. Nichols, J. C. T. Eijkel, and H. J. G. E. Gardeniers, *Lab. Chip*, **2007**, 8, 173.
- [30] W. Sparreboom, J. C. T. Eijkel, J. Bomer, and A. van den Berg, *Lab. Chip*, **2008**, 8, 402.
- [31] N. R. Tas, P. Mela, T. Kramer, J. W. Berenschot, and A. van den Berg, *Nano Lett.*, **2003**, 3, 1537.
- [32] R. Müller, P. Schmid, A. Munding, R. Gronmaier, and E. Kohn, *Diam. Relat. Mater.*, **2004**, 13, 780.
- [33] E. Herth, P. Tilmant, M. Faucher, M. François, C. Boyaval, F. Vaurette, Y. Debloq, B. Legrand, and L. Buchaillet, *Microelectron. Eng.*, **2010**, 87, 2057.

- 1 [34] F. Chauvet, P. Duru, S. Geoffroy, and M. Prat, *Phys.Rev.Lett*, **2009**, 110, 124.
2
3 [35] J.B. Laurindo and M. Prat, *Chem.Eng.Sci.*, **1998**, 53, 2257.
4
5 [36] J.C.T. Eijkel et al., *Phys.Rev.Lett.*, **2005**, 95, 256107.
6
7 [37] M. Prat et al., *Int.J.Heat.Mass.Transp.*, **2007**, 50, 1455.
8
9 [38] C. Duan, R. Karnik, M.-C.Lu, and A. Majumdar, *PNAS*, **2012**, 109, 3688.
10
11 [39] J. Lee, T. Laouiard, R. Karnil, *Nat.Nano*, **2014**, 9, 317.
12
13 [40] P. Joseph, et al., *MicroTAS*, **2010**, Groningen, the Netherlands.
14
15 [41] J.C.T. Eijkel, and A. van den Berg, *Lab.Chip.*, **2005**, 5, 1202.
16
17 [42] H.J. Crabtree, et al., *Anal.Chem*, **2001**, 73, 4079.
18
19 [43] R.D. Deegan et al., *Nature*, **1997**, 389, 827.
20
21 [44] K. Roger, M. Liebi, J. Heimdal, Q.D. Pham, and E. Sparr, *PNAS*, **2016**, 113, 10275.
22
23 [45] N. Shokri, P. Lehman and D.Or, *Geophys.Res.Lett.*, **2008**, 35, L19407.
24
25 [46] S.Yu et al, *Sci.Rep.*, **2015**, 5, 13600.
26
27 [47] R.Sordan et al, *Lab.Chip.*, **2009**, 9, 1556.
28
29 [48] S.Jeon et al, *Nanolett.*, **2005**, 5, 1351.
30
31 [49] S.Liao et al, *Lab.Chip.*, **2013**, 13, 1626.
32
33 [50] N.Clement, G. Patriarche, K. Smaali, F. Vaurette, K. Nishiguchi, D. Troadec, A.
34 Fujiwara and D. Vuillaume, *Small*, **2011**, 7, 2607.
35
36 [51] K.Smaali, et al., *ACS Nano*, **2012**, 6, 4639.
37
38 [52] K.Smaali, et al., *Nanoscale*, **2015**, 7, 1809.
39
40 [53] J. Trasobares, et al., *Nat.Comm.*, **2016**, 7, 12850.
41
42 [54] N.Clement, et al., *Nanolett.*, **2013**, 13, 3903.
43
44 [55] H.Cai, et al., *ACS Nano.*, **2016**, 10, 4173.
45
46 [56] N.Clement, et al., *Appl.Phys.Lett.*, **2011**, 98, 014104.
47
48 [57] R. Sivakumarasamy et al., *Selective-layer-free Blood Ionogram using a Nanoscale*
49
50
51
52
53
54
55
56
57
58
59
60
61 *Silicon Transistor that breaks the Boltzmann ion distribution*
62
63
64
65

[58] C.A. Nijhuis et al., *Nanolett.*, **2010**, 10, 3611.

1
2
3
4
5
6
7
8
9
10
11
12
13
14
15
16
17
18
19
20
21
22
23
24
25
26
27
28
29
30
31
32
33
34
35
36
37
38
39
40
41
42
43
44
45
46
47
48
49
50
51
52
53
54
55
56
57
58
59
60
61
62
63
64
65

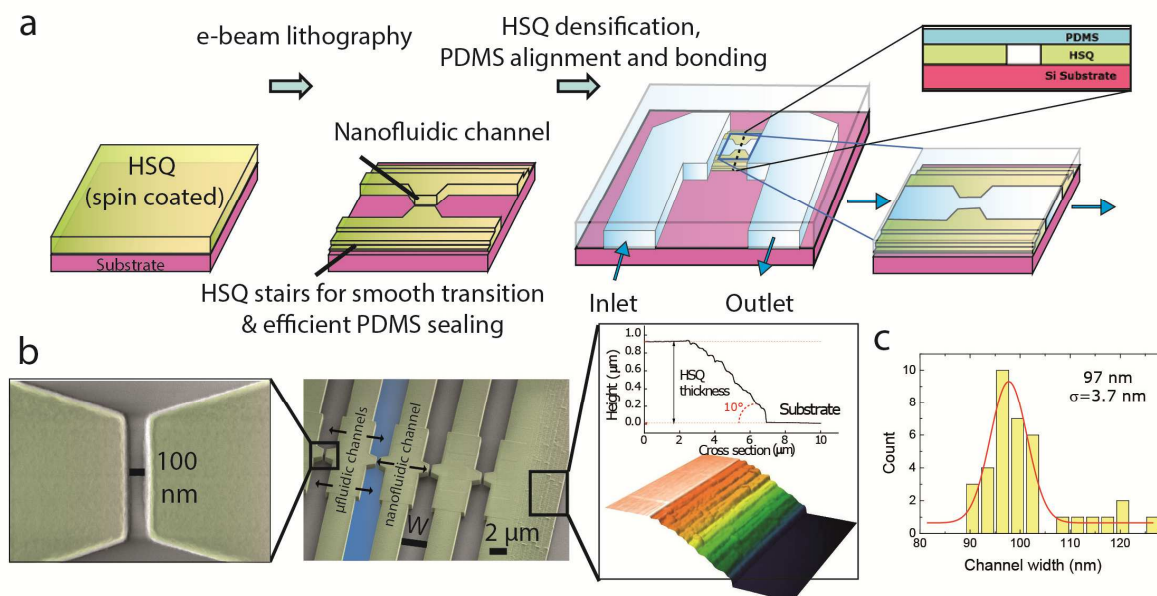


Figure 1. HSQ-based nanofluidics with direct HSQ patterning and PDMS bonding

(a) Schematic view of the HSQ-based fabrication process. 850 nm-thick HSQ is first spin-coated. HSQ walls and stairs are written within a unique and short e-beam lithography step (typically 1 min/chip). HSQ is baked on a hot plate for 30 min at 110°C , followed by 30 min at 180°C and the PDMS microfluidic channel is then aligned and bonded. (b) Scanning Electron Microscope (SEM) top views of the HSQ nanochannels and Atomic Force Microscope topography image of HSQ stairs with a cross section. Channel width W is $3\ \mu\text{m}$ at inlets and outlets and below $100\ \text{nm}$ at the nanoconstriction that defines the nanofluidic channel. (c) Histogram of nanofluidic channel width measured by SEM for 37 channels. Average width is $97\ \text{nm}$ with a standard deviation $\sigma = 3.7\ \text{nm}$.

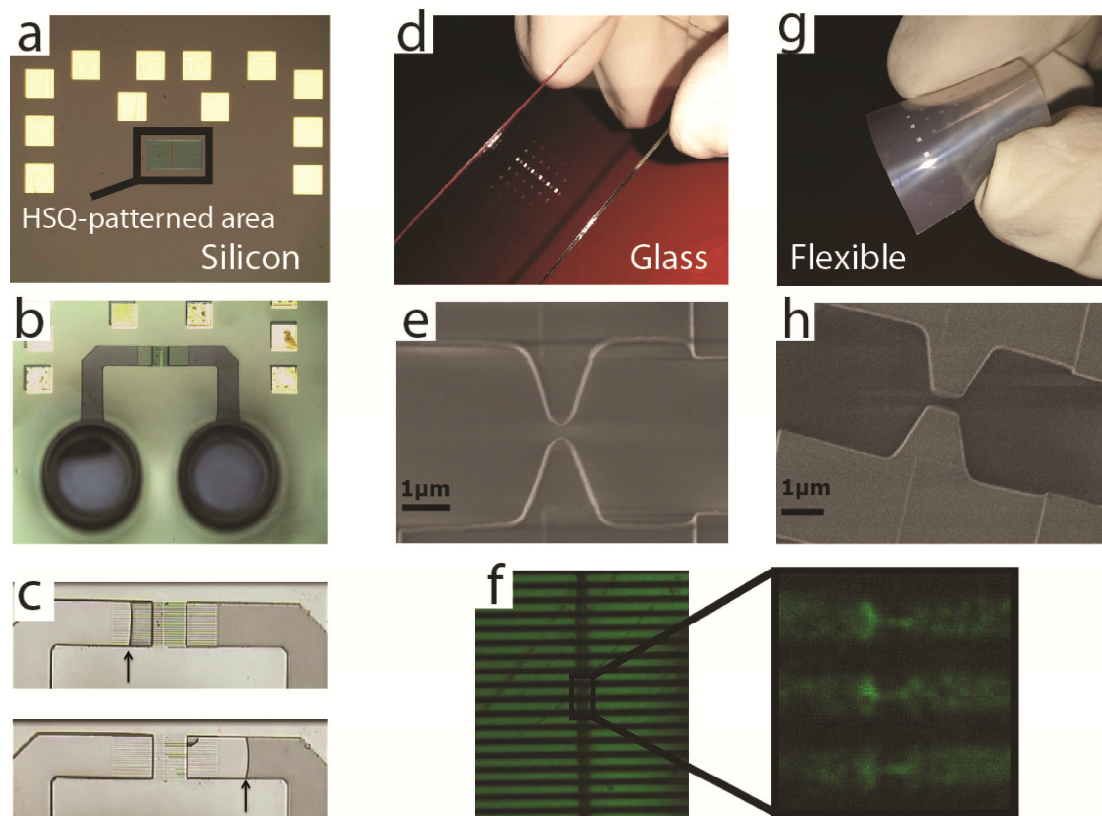


Figure 2. Versatility of HSQ-based nanofluidics

(a- c) Silicon substrate: (a) Optical image showing the HSQ-patterned area. (b) Microfluidic channels aligned on the HSQ patterned area to form a microfluidic/nanofluidic transition. (c) Demonstration of flow of DI water in the nanofluidic channels (water progress and the direction of the flow are indicated by an arrow). Transparent color corresponds to filled channels. Applied pressure was 3 bars. (d-f) HSQ-based nanofluidics on glass substrate: (d) Picture of the glass slide with HSQ-patterned areas. (e) SEM image of the HSQ nanoconstriction. (f) Confocal microscope image of the nanofluidic channels filled with Alexa-marked 25 ss-DNA. (g-h) HSQ-based nanofluidics on flexible substrate: (g) Picture of the flexible substrate with HSQ-patterned areas. (h) SEM image of the HSQ nanoconstriction.

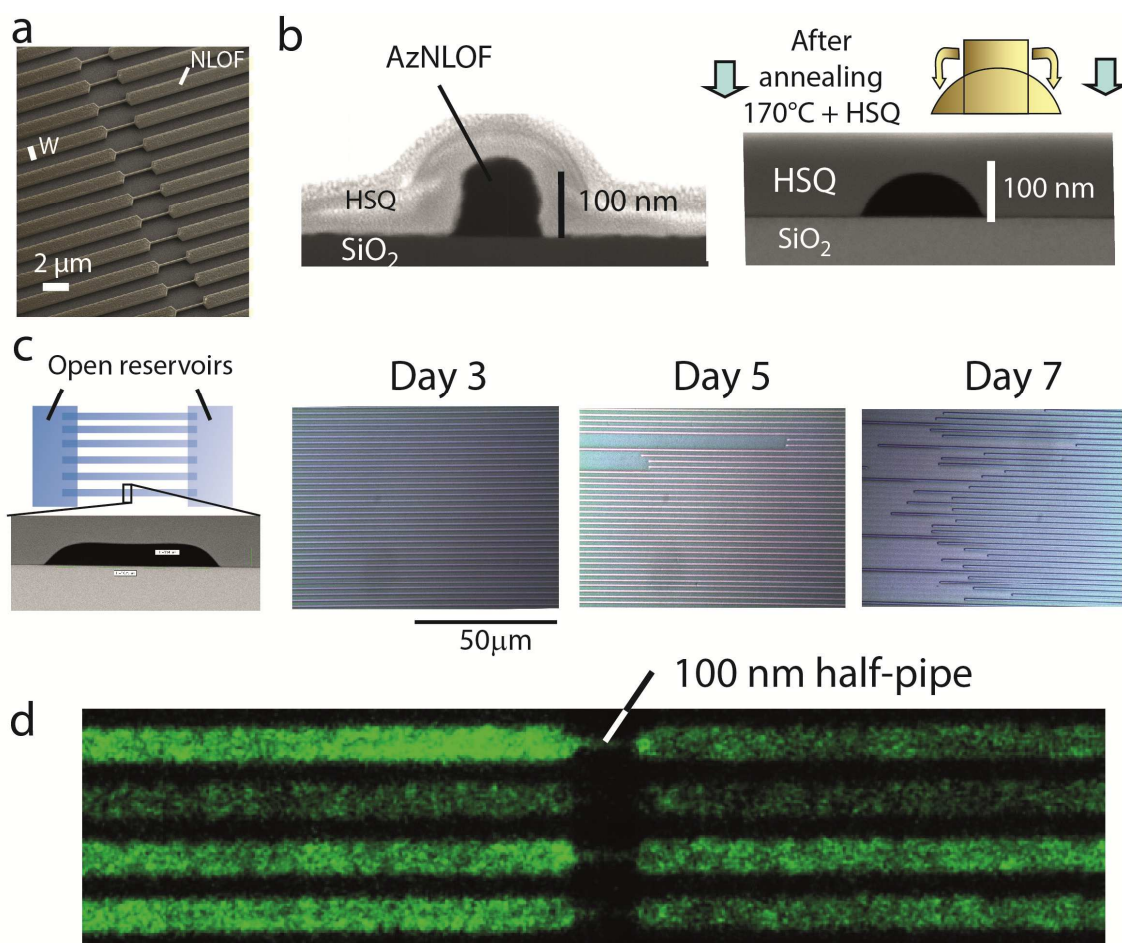


Figure 3. HSQ-based nanofluidics with sacrificial layer approach

(a) SEM image (top view) of the AZnLof sacrificial layer. (b) Cross sectional SEM image of nanochannels before annealing (left) and after the complete process including sacrificial layer removal (right). (c) Study of the evaporation rate. Left: schematic view of the nanofluidic channels (3 μm wide, 100 nm thick) nanofluidic channels with open reservoirs. The related cross-section SEM image is shown below. Right: Optical images of the nanofluidic channels showing the extremely slow evaporation rate over 1 week (<1 fL/h starting after day 4). The pictures have not been taken on the structure center (slightly on the left) for showing evaporation coming only from the sides. (d) Confocal microscope image of ss-DNA marked with Alexa fluorophore.

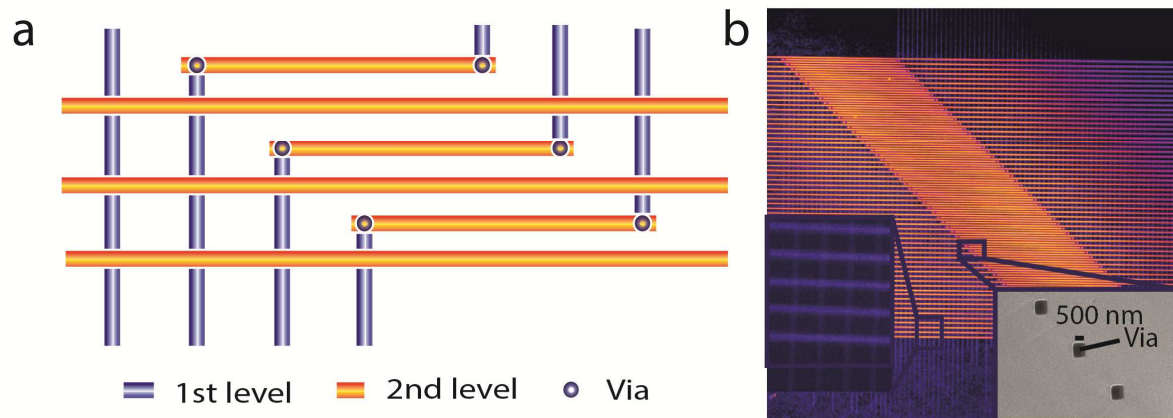


Figure 4. 3D HSQ-based nanofluidics

a) Schematic representation of the 3D nanofluidics structure. b) Related confocal microscope image of the 3D nanofluidics channels with ss-DNA marked with Alexa fluorophore. Inset: SEM image of the vias used for the 3D nanofluidics channels.

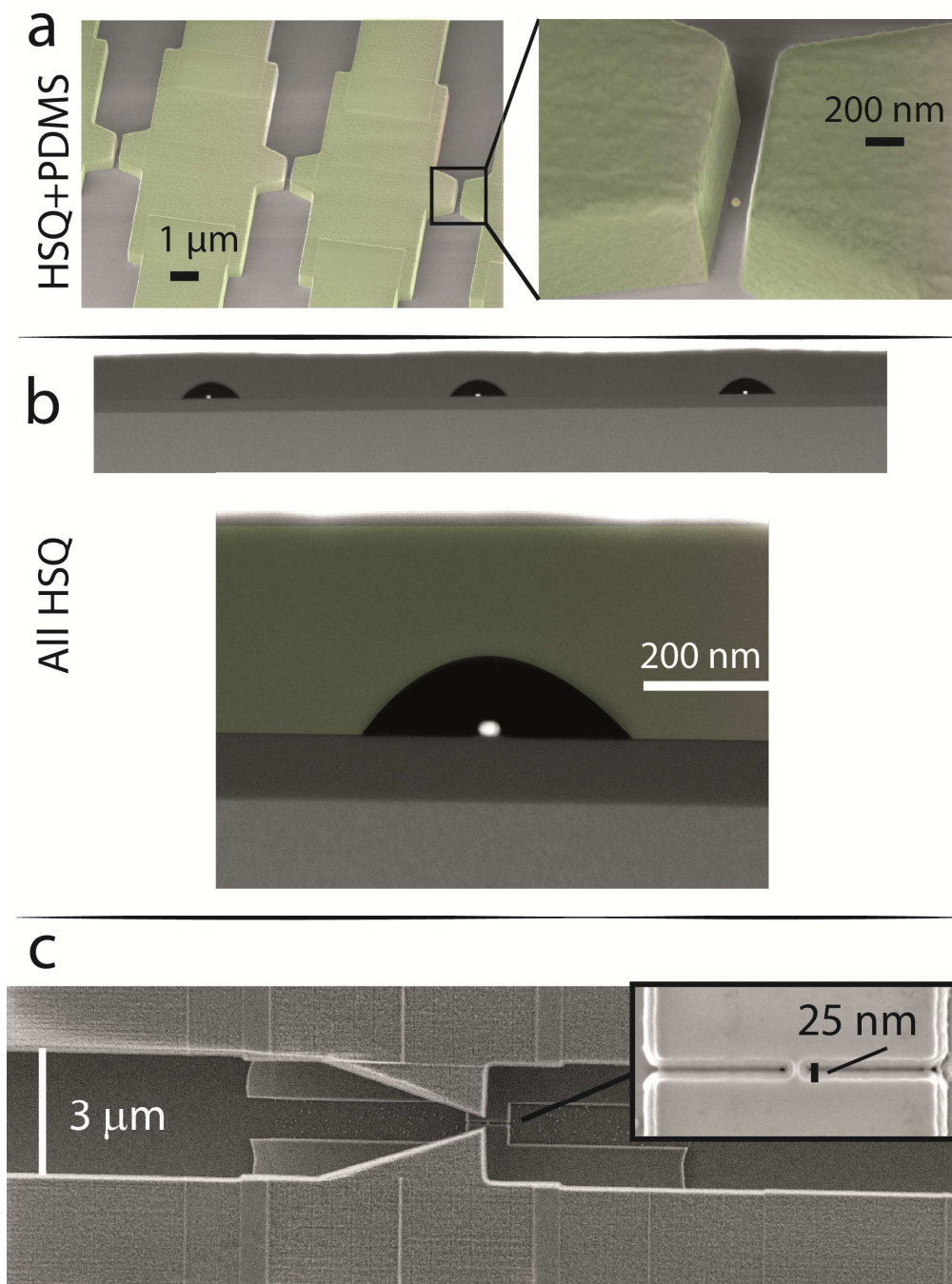
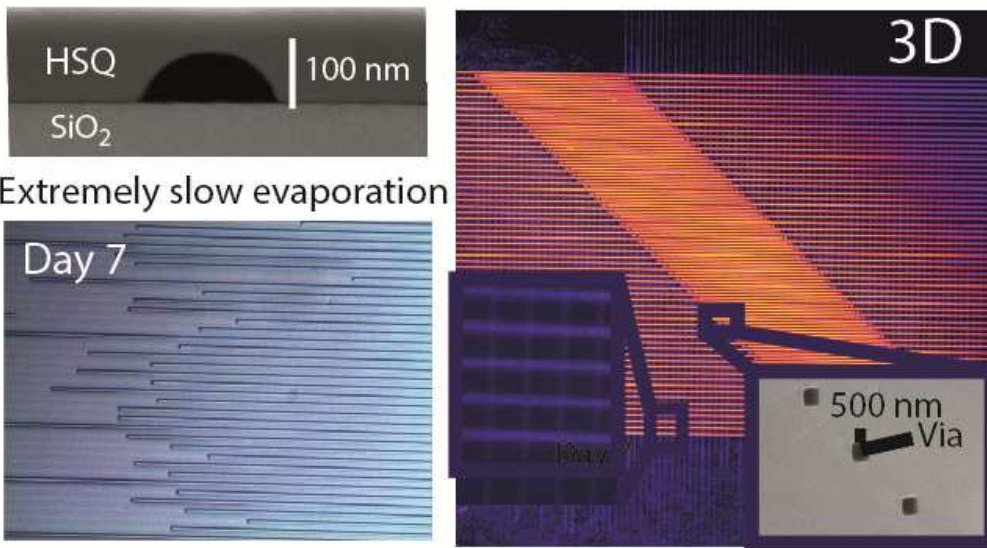


Figure 5. Nanochannels with nanometric alignment precision ability

a) SEM image of the nanofluidics channels aligned on 20 nm-large gold nanodot (fabricated with the direct patterning of HSQ). b) SEM cross section images of nanofluidics channels fabricated with the sacrificial layer approach with precisely aligned gold nanoparticles. c) SEM top view of an HSQ-based nanofluidic channel aligned on a patterned surface, namely a nanoscale transistor biosensor. Inset: SEM image of the nanoscale transistor biosensor.

Hydrogen Silsesquioxane-based Nanofluidics

ToC figure



1
2
3
4
5
6
7
8
9
10
11
12
13
14
15
16
17
18
19
20
21
22
23
24
25
26
27
28
29
30
31
32
33
34
35
36
37
38
39
40
41
42
43
44
45
46
47
48
49
50
51
52
53
54
55
56
57
58
59
60
61
62
63
64
65

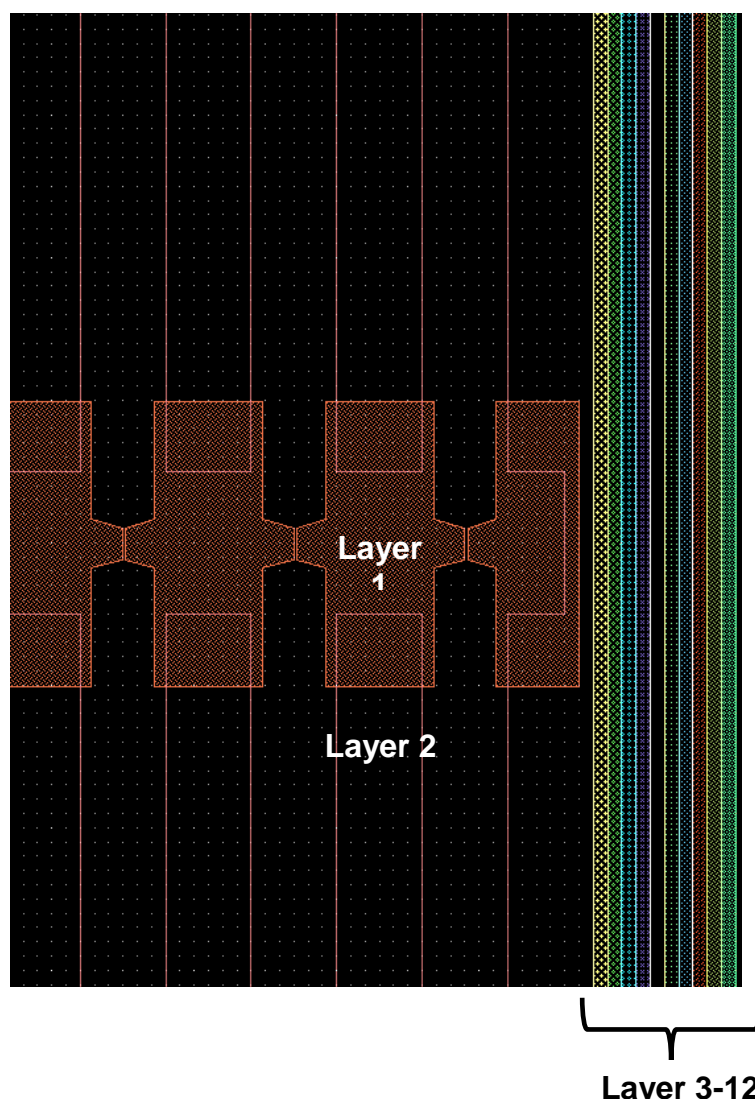
Copyright WILEY-VCH Verlag GmbH & Co. KGaA, 69469 Weinheim, Germany, 2013.

Supporting Information

Hydrogen Silsesquioxane-based Nanofluidics

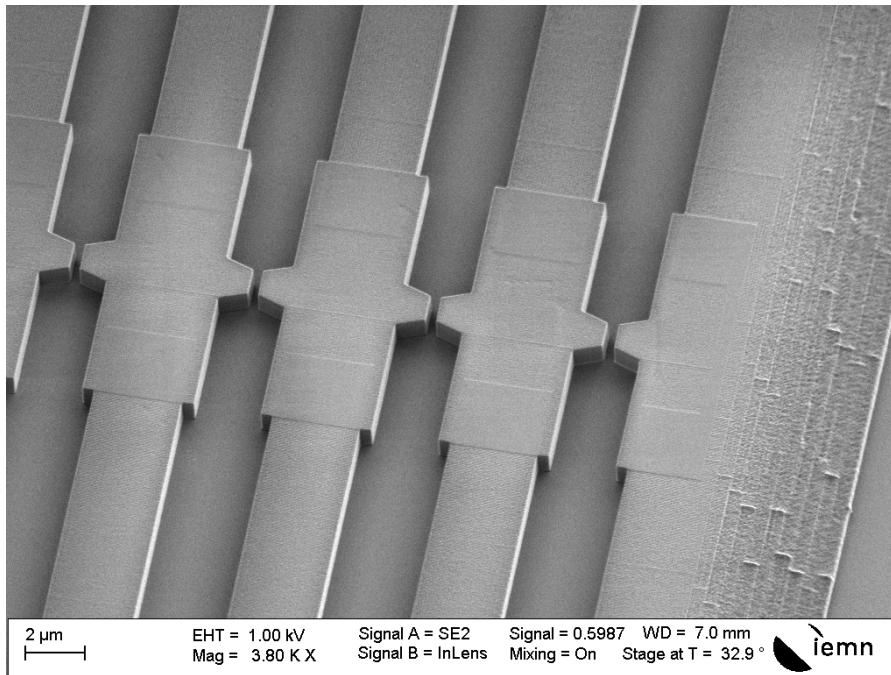
*Sathyanarayanan Punniyakoti, Ragavendran Sivakumarasamy, Francois Vaurette, Pierre Joseph, Jean-Francois Dufreche, and Nicolas Clément**

3D prototyping of HSQ

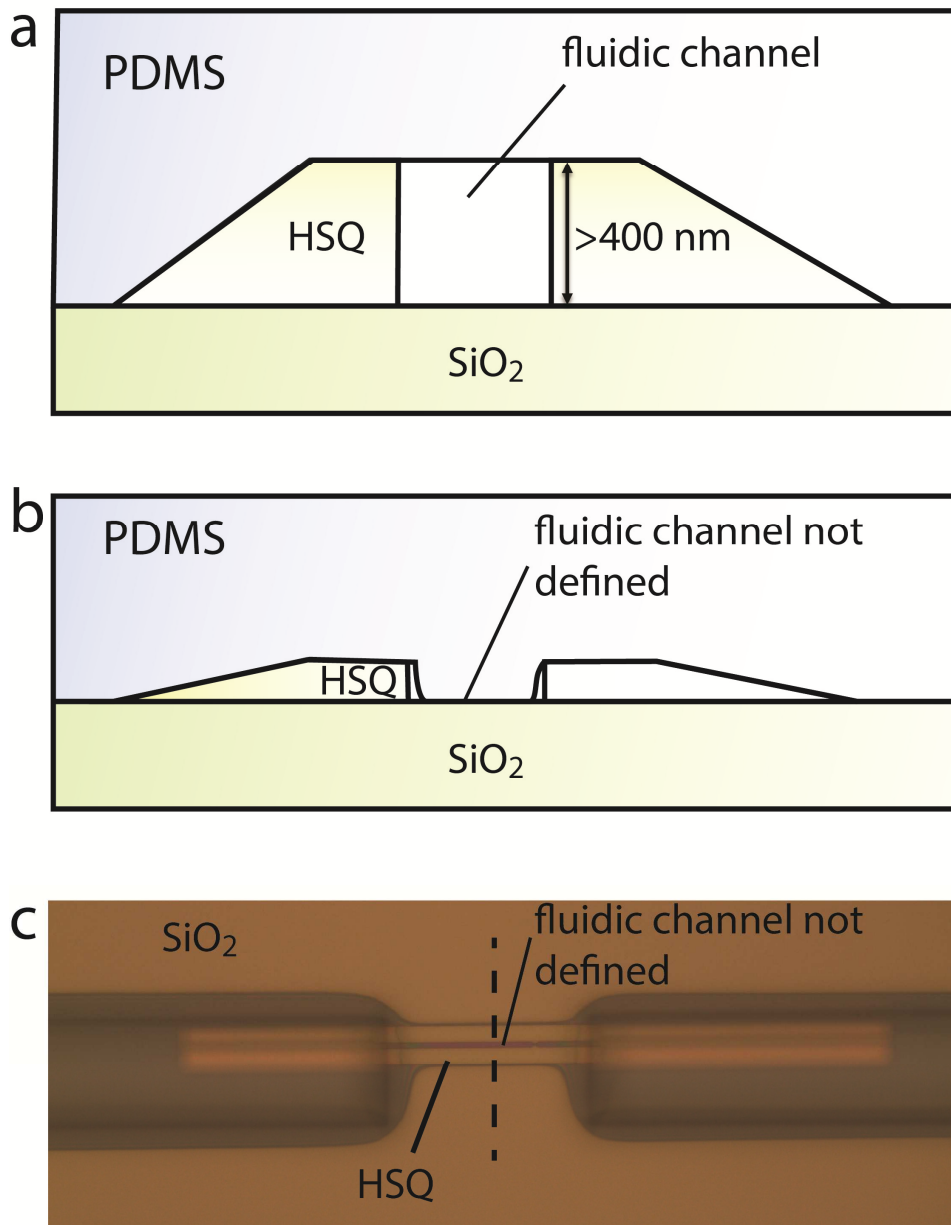


Supplementary Fig.1: Layout of the structure shown in Fig.1. Layer 1 is performed at High resolution, and layers 2-12: at low resolution. Doses in $\mu\text{C}/\text{cm}^2$ were 850,1000,900,800,750,700,650,600,575,550,525,500 respectively.

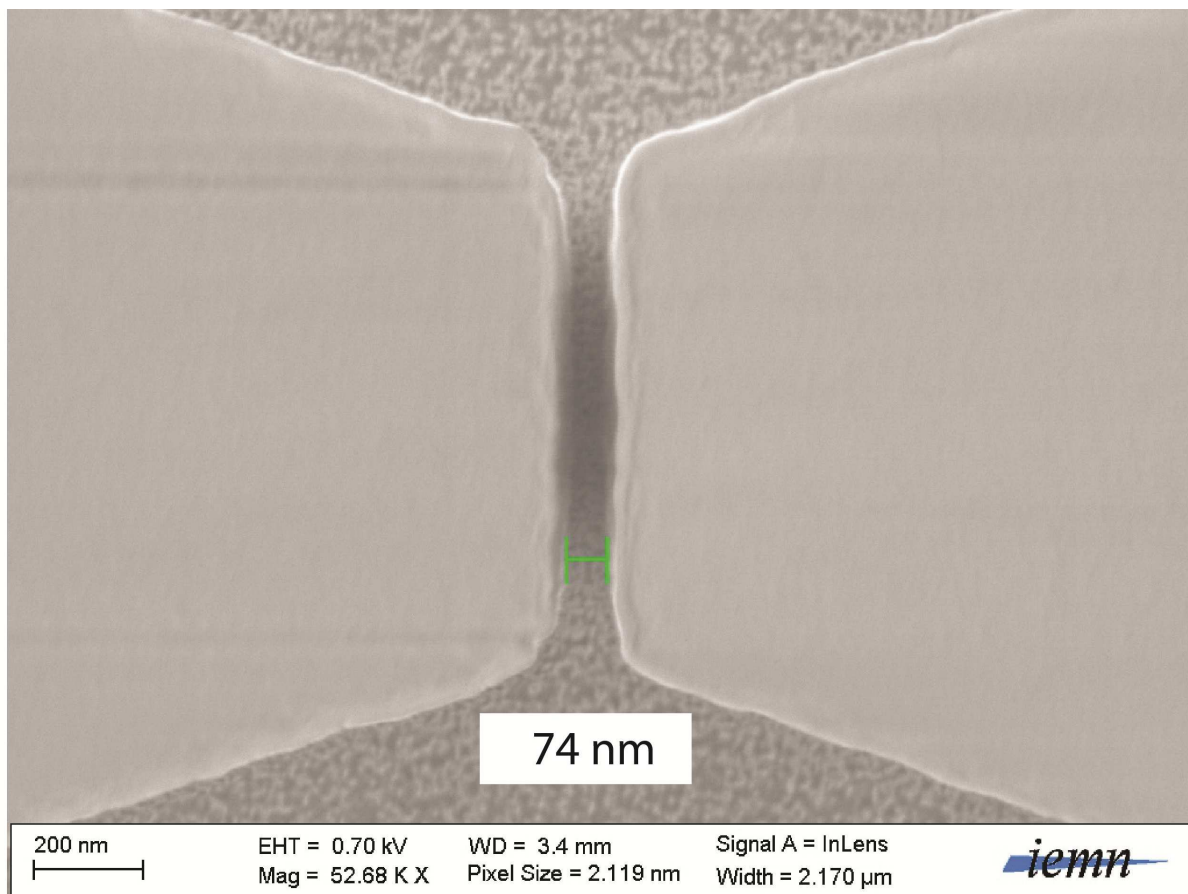
Electron beam lithography: Raith EBPG 5000P



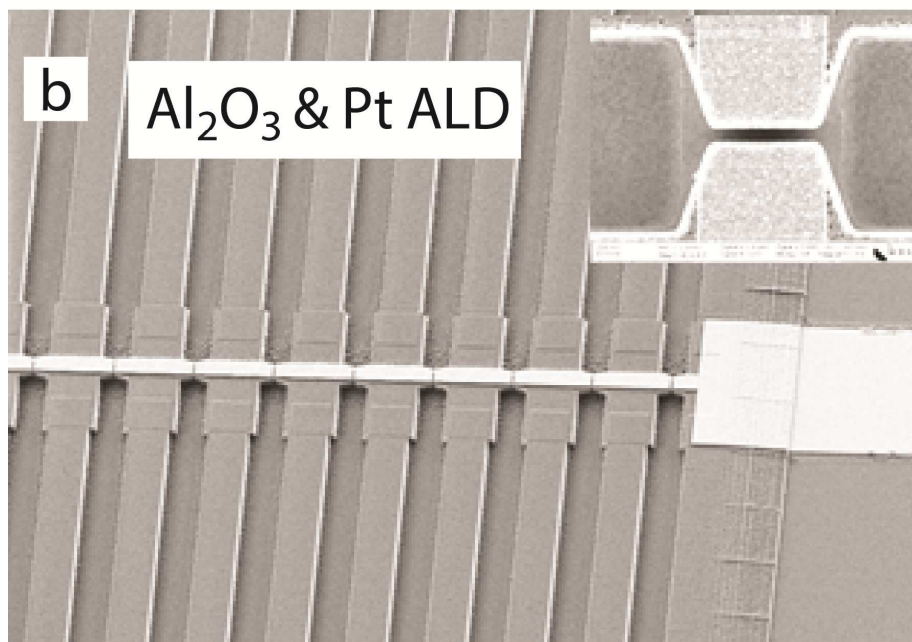
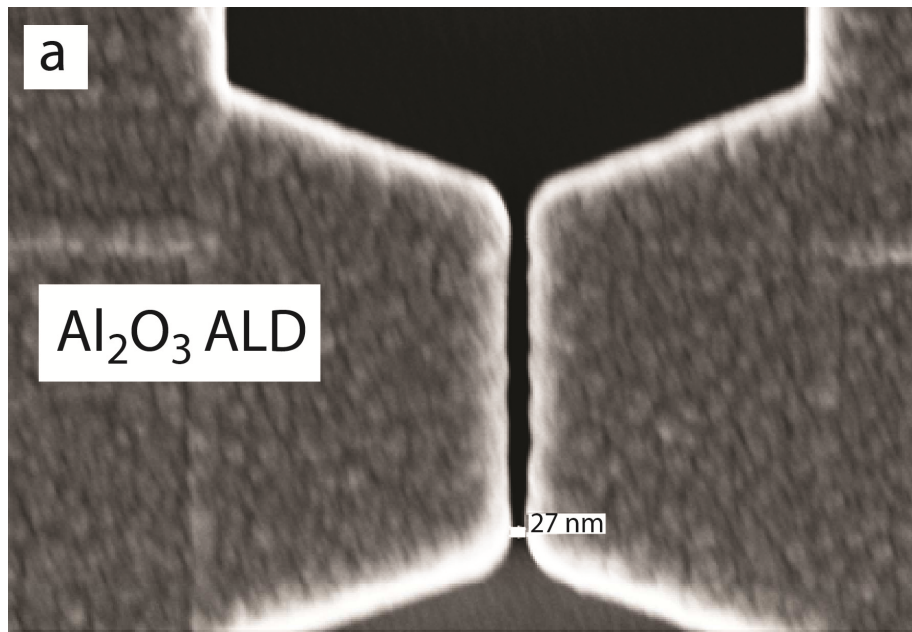
Supplementary Fig.2: E-beam lithography (Raith EBPG 5000P) corresponding to the layout shown in Supplementary Fig.1.



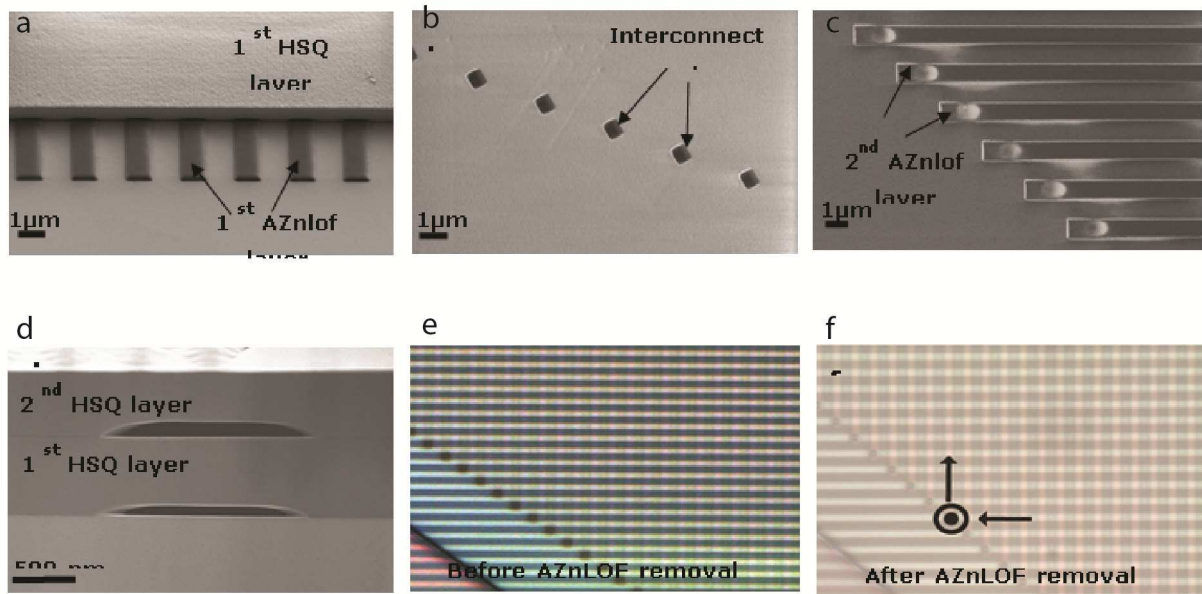
Supplementary Fig.3: Illustration of the minimum HSQ layer thickness required. a) Schematic representation of the efficient process when the HSQ layer thickness is above 400 nm. The fluidic channel is well defined. b) Schematic representation of the process when a thin HSQ layer is used. The PDMS bonds in the channel and the fluidic channel is not defined. c) Optical microscope image corresponding to the schematic representation in b) for a 300 nm thick HSQ layer.



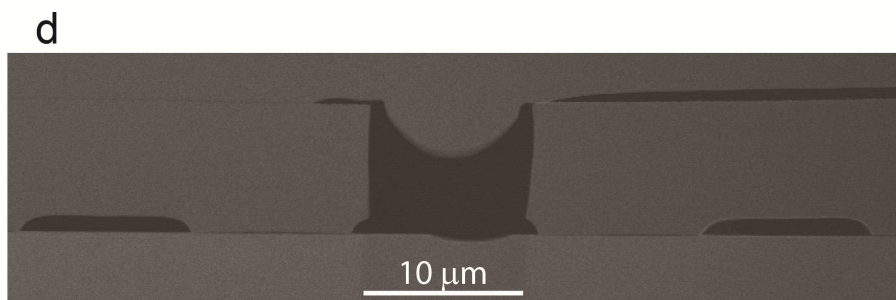
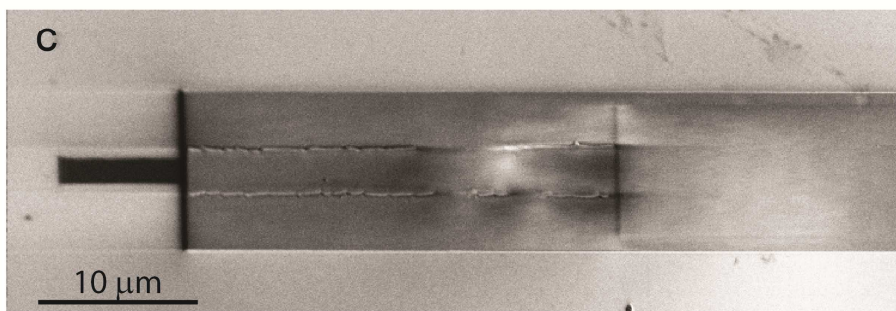
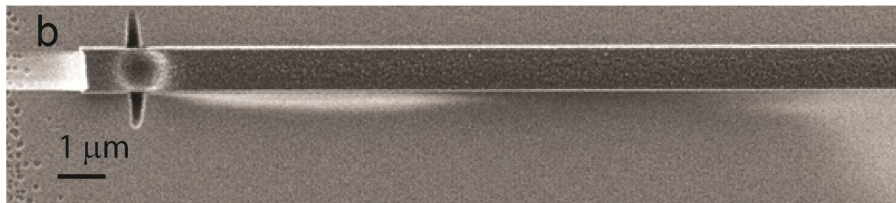
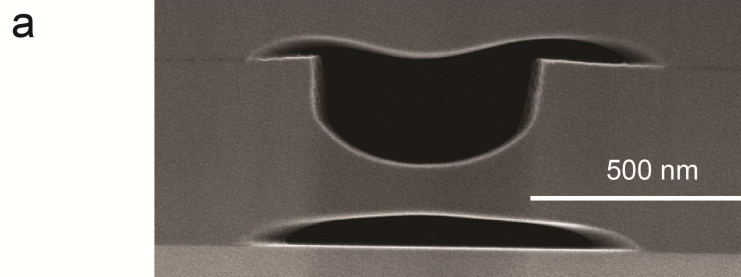
Supplementary Fig.4: Illustration of the minimum HSQ channel width obtained for an HSQ layer thickness of 850 nm.



Supplementary Fig.5: Tuning channel width and properties using ALD. a) SEM image showing a channel <30 nm obtained after ALD of Al_2O_3 . b) SEM image of the nanofluidic channels composed of HSQ/ Al_2O_3 /Pt/ Al_2O_3 , which could be used for the development of vertical nanofluidic transistors. Inset: Top view image.



Supplementary Fig.6: Step-by-step explanation of the 3D HSQ nanofluidics. a) standard process for layer 1. b) Vias aligned on layer 1. c) Second layer of AzNLOF. d) Cross section image after 2 layers deposition (channels are tilted to their main axis to get both channels on the same cross section). e) Optical image before sacrificial layer removal. f) Optical image after AznLOF removal.



44
45
46
47
48
49
50
51
52
53
54
55
56
57
58
59
60
61
62
63
64
65

Supplementary Fig.7: Issues to be considered as design rules for (3D) HSQ nanofluidics. a) SEM image illustrating the difficulty of achieving a uniform etching of the via. b) SEM image showing a crack appearing in HSQ if the etching time is above the AznLof layer. c) SEM image showing the collapse of HSQ if the channel width is above 3 μm or if the HSQ layer thickness is below 400 nm. d) SEM image showing that the 2nd layer of AZnLOF can fall into the via, which can induce a clogging of the hole after HSQ deposition. A 500 nm large via is the best compromise.